

The Interaction of Calcium and Metabolic Oscillations in Pancreatic β -cells

REU Site: Interdisciplinary Program in High Performance Computing

Mary Aronne¹, Samantha Clapp², Soohwan Jung³, Abigail Kramer⁴, William Wang⁵,
Graduate assistant: Janita Patwardhan¹, Faculty mentor: Bradford E. Peercy¹, and
Client: Arthur Sherman⁶

¹Department of Mathematics and Statistics, UMBC,

²Department of Mathematics, Georgia College and State University,

³Department of Mathematics, Edmonds Community College,

⁴Department of Mathematical Sciences, Kent State University,

⁵Department of Mathematics, Vanderbilt University,

⁶Laboratory of Biological Modeling, National Institutes of Health

Technical Report HPCF-2016-14, hpcf.umbc.edu > Publications

Abstract

Diabetes is a disease characterized by an excessive level of glucose in the bloodstream, which may be a result of improper insulin secretion. Insulin is secreted in a bursting behavior of pancreatic β -cells in the islets of Langerhans, which is affected by oscillations of cytosolic calcium concentration. We used the Dual Oscillator Model to explore the role of calcium in calcium oscillation independent and calcium oscillation dependent (CaD) modes as well as the synchronization of metabolic oscillations in electrically coupled β -cells. We also implemented a synchronization index in order to better measure the synchronization of the β -cells within an islet. We observed that voltage or calcium coupling result in increased synchronization and are more effective in CaD modes. Furthermore, we studied heterogeneous modes of coupled β -cells, their arrangements in the islets, and their synchronization. We saw that increasing calcium coupling or increasing voltage coupling in heterogeneous cases increases synchronization; however, in certain cases increasing both voltage and calcium coupling causes desynchronization, primarily in voltage. To better represent an entire islet, we altered previous code by further optimizing run-time and memory usage to allow for a greater number of cells to be simulated for a longer period of time.

Key words. pancreatic β -cells, islet, calcium, metabolic oscillations, Dual Oscillator Model, Synchronization Index

1 Introduction

Insulin is a hormone secreted by pancreatic β -cells that manages blood plasma glucose levels. Improper insulin secretion can result in chronically elevated levels of glucose in the bloodstream in a disease known as diabetes. Diabetes can lead to kidney failure, blindness, limb amputation, cardiovascular disease, and death [3]. There are two types of diabetes; Type I involves an autoimmune destruction of β -cells which results in a complete absence of insulin. Type II involves a deficiency of insulin caused by insulin resistance as well as a failure of β -cells to produce enough insulin to compensate. Type II is the more common form of diabetes, with a rising number of cases concentrated in industrialized countries [3]. The rise in diabetes has driven research to better understand β -cells.

Our research focuses on understanding β -cells by investigating calcium oscillation independent (CaI) and calcium oscillation dependent (CaD) modes. We do this through exploring the effects of voltage and calcium coupling as well as different types heterogeneous cellular bursting arrangements on the synchronization of cells in these modes. We have arranged our report as follows. In Section 2 there is a brief overview of the physiology of β -cells as well as the Dual Oscillator Model. The methodology is described in Section 3 and the results are described in Section 4. The conclusions of our research are drawn in Section 5.

2 Background

2.1 Physiology

In the pancreas, the endocrine cells are found in clusters called islets of Langerhans [3]. The islet consists of α , β , and δ cells; β -cells are responsible for insulin secretion. The process of insulin secretion begins when glucose enters a β -cell. Glycolysis starts, during which adenosine diphosphate (ADP) is converted to adenosine triphosphate (ATP). The ratio of ATP to ADP increases, causing the ATP dependent potassium channels (K_{ATP}) to close and the β -cell to depolarize. As a result, the calcium (Ca^{2+}) channels open, allowing Ca^{2+} to flow into the cytoplasm from the outside of the cell. The increase in Ca^{2+} triggers the endoplasmic reticulum (ER) to open its large Ca^{2+} store, leading to a higher concentration of Ca^{2+} in the cell. Due to this greater concentration, insulin is released into the bloodstream through exocytosis. The ATP/ADP ratio is restored by exocytosis and other cell functions, such as the calcium pump that expels excess Ca^{2+} , lowering the concentration. The K_{ATP} channel is reopened and the cell is repolarized, resetting the β -cell.

The process of the calcium channels opening and closing results in calcium oscillations, whereas the flow of ions in and out of the cell lead to voltage oscillations. During process of glycolysis, there is a positive feedback loop of fructose 1,6-bisphosphate (FBP) on phosphofructokinase (PFK) causing the production of more FBP until fructose 6-phosphate (F6P) is depleted, which causes PFK activity to stop until F6P levels recover. This process causes

metabolic oscillations. There are different flux of glucokinase (J_{GK}) values that determine whether a cell is CaI or CaD. If it depends on the calcium oscillation levels, it is CaD, and if it does not depend on the calcium oscillation levels, it is CaI. The range of CaD is from $0.01 J_{GK}$ to $0.176 J_{GK}$. The range of CaI is from $0.045 J_{GK}$ to $0.15 J_{GK}$. Ca^{2+} links the electrical and metabolic oscillations that are exhibited by β -cells in response to elevated glucose levels in the bloodstream. Together these two oscillations regulate the secretion of insulin by the β -cells. Each time an oscillation completes is considered a burst representing one cycle of insulin secretion. β -cells can be classified into two categories, slow and fast, based upon their bursting periods. Slow bursting β -cells burst approximately every four to six minutes. Fast bursting β -cells burst approximately every ten seconds [2]. In islets however, there is a mix of differently bursting cells called heterogeneity. The timing of the insulin secretion process is dependent on the (J_{GK}) value of the cell.

The β -cells do not act independently to release insulin. They are connected by gap junctions, which are proteins split between the cell membranes that allow small molecules to travel from cell to cell. Gap junctions impact the voltage between cells as well as Ca^{2+} concentration in each cell. A transmembrane current is created across the gap junction due to the flow of ions between cells [3]. As the process of insulin secretion happens for one cell, it is signaled to the connecting cells and the bursting is synchronized [2].

In healthy cells insulin secretion is oscillatory; however, in pre-diabetic subjects these oscillations do not occur. It is possible that the lack of oscillations are connected with desynchronization of β -cells in an islet. This is thought because in an islet when β -cells are not synchronized, insulin secretion in an islet does not oscillate.

2.2 Dual Oscillator Model

The Dual Oscillator Model (DOM) [6] represents the process of insulin secretion for a single β -cell by seven differential equations consisting of three components: electrical, mitochondrial, and glycolytic.

$$\frac{dV}{dt} = -\frac{I_K + I_{Ca} + I_{K(Ca)} + I_{K(ATP)}}{C_m} \quad (2.1)$$

$$\frac{dn}{dt} = \frac{n_\infty(V) - n}{\tau_n} \quad (2.2)$$

$$\frac{d[Ca]}{dt} = f_{cyt}(J_{mem} + J_{er}) \quad (2.3)$$

$$\frac{d[Ca_{er}]}{dt} = -\sigma_V f_{er} J_{er} \quad (2.4)$$

$$\frac{d[ADP]}{dt} = J_{hyd} - \delta J_{ANT} \quad (2.5)$$

$$\frac{d[G6P]}{dt} = k(J_{GK} - J_{PFK}) \quad (2.6)$$

$$\frac{d[FBP]}{dt} = k(J_{PFK} - \frac{1}{2}J_{GPDH}) \quad (2.7)$$

Equations (2.1) through (2.4) contain the electrical model, equation (2.5) describes the cell's mitochondrial activity, and equations (2.6) and (2.7) represent glycolytic activity. I_i indicates the ionic currents through the specific channels where $i \in \{K, Ca, K(Ca), K(ATP)\}$. Note that I_K and I_{Ca} are voltage dependent, $I_{K(Ca)}$ is Ca^{2+} -activated, and $I_{K(ATP)}$ is sensitive to the ATP/ADP ratio. V shows the membrane potential and C_m represents the membrane capacitance. In equation (2.2), n is the activation variable for the voltage dependent K channel. J_x serves to show flux where $x \in \{mem, er, hyd, ANT, GK, PFK, GPDH\}$. The volume fraction of the relationship between the ER and the cytoplasm is given by σ_V as seen in equation (2.4).

The following equations, (2.8) through (2.11), use Ohm's law and form the basis for equation (2.1). g_i is the conductance where as \bar{g}_i represents the maximal conductance for the respective current.

$$I_K = \bar{g}_K n (V - V_K) \quad (2.8)$$

$$I_{Ca} = \bar{g}_{Ca} m_\infty (V - V_{Ca}) \quad (2.9)$$

$$I_{K(Ca)} = g_{K(Ca)} (V - V_K) \quad (2.10)$$

$$I_{K(ATP)} = g_{K(ATP)} (V - V_K) \quad (2.11)$$

The activation variables n and m are given by

$$n_\infty(V) = \frac{1}{1 + e^{-(16+V)/5}} \quad (2.12)$$

$$m_\infty(V) = \frac{1}{1 + e^{-(20+V)/12}}. \quad (2.13)$$

The K(Ca) conductance in (2.14) is given by an increasing sigmoidal function of the Ca^{2+} concentration and the K(ATP) conductance in (2.15) is dependent on the ADP and ATP

concentrations, where the conductance function O_∞ is given by the Magnus-Keizer expression [1].

$$g_{K(Ca)} = \bar{g}_{K(Ca)} \left(\frac{Ca^2}{K_D^2 + Ca^2} \right) \quad (2.14)$$

$$g_{K(ATP)} = \bar{g}_{K(ATP)} O_\infty(ADP, ATP) \quad (2.15)$$

The free cytoplasmic calcium concentration $[Ca]$ in equation (2.3) uses the fraction of free to total cytosolic Ca^{2+} (f_{cyt}) along with equations (2.16) through (2.19).

$$J_{mem} = -(\alpha I_{Ca} + k_{PMCA}[Ca]) \quad (2.16)$$

$$J_{er} = J_{leak} - J_{SERCA} \quad (2.17)$$

$$J_{leak} = p_{leak}([Ca_{er}] - [Ca]) \quad (2.18)$$

$$J_{SERCA} = k_{SERCA}[Ca] \quad (2.19)$$

These equations describe the flux of Ca^{2+} across the membrane (J_{mem}), the flux of Ca^{2+} out of the endoplasmic reticulum (J_{er}), leakage permeability (p_{leak}), and SERCA pump rate (k_{SERCA}). In equation (2.16), α converts current to flux and k_{PMCA} is the Ca^{2+} pump rate. In our reduced model, only the leakage (J_{leak}) leads to flux out of the ER, and only the SERCA pumps (J_{SERCA}) lead to Ca^{2+} flux into the ER.

2.3 Coupling

Coupling of N^3 cells is considered to better understand the way β -cells interact in islets through gap junctions. To couple multiple cells in an islet, we created a diagonal coupling matrix G , which connects the voltages and calcium concentrations between a cell and its neighboring cells. We construct a vector,

$$y = \begin{bmatrix} V_i \\ n_i \\ [Ca]_i \\ [Ca_{ER}]_i \\ [ADP]_i \\ [G6P]_i \\ [FBP]_i \end{bmatrix}, \text{ where } i = 1 \text{ to } N, \quad (2.20)$$

that contains these values for all of the cells. We now define our system of ODEs to be

$$\frac{dy}{dt} = f(t, y) + Gy$$

where $f(t, y)$ encompasses the happenings inside each cell taken from the DOM and Gy accounts for the adjusted behavior of the β -cells due to coupling.

3 Numerical Methods

The DOM can be examined two ways: as a single cell model and as an islet model. The single cell model shows how one β -cell reacts to electrical and metabolic oscillations represented in equations (2.1)-(2.7). The islet model replicates this single cell model for N^3 cells then uses the coupling matrix G to consider how the cells interact. Both models are based on Matlab files used in previous work at University of Maryland, Baltimore County High Performance Computing Facility [2]. This file was adapted from Bertram’s XPPAUT file that implemented the DOM [1].

3.1 Islet Model

The islet is modeled as a cube of $N \times N \times N$ cells with indexing (i, j, k) . For computational purposes, the values associated with each cell are stored in a vector y , in equation (2.20). The indexing is given as $l = i + N(j - 1) + N^2(k - 1)$ to access the (i, j, k) th element in y . To compute the impact of coupling on each cell, the C matrix shows the influence of the surrounding cells on each individual cell. C is a matrix of coupling coefficient values that is modified to account for the chosen coupling values in C' . G is a box diagonal matrix, with each box on the diagonal containing C' . Each row represents the effects of connecting cells to one cell. If the m th and n th cells are not connected, then the (m, n) and (n, m) entries of the matrix will be zero; if they are connected, the entries will be their coupling relation. The diagonal of matrix C is the number of neighboring cells multiplied by the coupling value, g . More information on the coupling matrix can be found in [4].

To accurately represent an islet, the initial values of each cell are taken from a normal distribution around the average value with standard deviation 20% of that average value. This allowed the initial values of each cell to be chosen within a certain range of the mean to see how the cell bursts synchronize. We took into account the heterogeneity of an islet and used three different patterns as seen in Figures 3.1, 3.2, and 3.3. The equal pattern in Figure 3.1 alternated between two J_{GK} values from cell to cell. In Figure 3.2, we see a layers pattern where each row alternates the J_{GK} values. The last pattern we modeled is called a layered split pattern that alternated between half rows of J_{GK} values seen in Figure 3.3. Within these patterns, we used various combinations of J_{GK} values in CaD and CaI ranges.

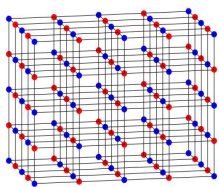


Figure 3.1: Equal-50-Percent

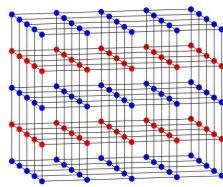


Figure 3.2: Layers

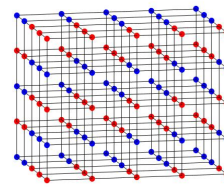


Figure 3.3: Layered-split

3.2 Optimizing the Numerical method

To obtain numerical solutions for the DOM, we chose the built-in Matlab solver `ode15s`, which can solve stiff differential equations in the form $My' = F(t, y)$. This particular solver is based on numerical differentiation formulas and efficiently solves large sets of equations at each time step. It effectively uses a mass symbolic Jacobian matrix obtained directly from the DOM code through the streamlined means of Matlab's Automatic Differentiation. We implemented a modified version of `ode15s` to optimize runtime and memory usage specifically for the DOM [4].

For simulations of a large N or high end time, the output is too large to write a MAT-file. To overcome this issue, we added a loop into the code that would run the simulation for a given amount of time and save the results in a MAT-file. Then the end value is taken as the new initial condition and the simulation is run for the next time period, saving these results in a new MAT-file. We call this loop the Time Interval Loop (TIL).

3.3 Synchronization Index

In order to quantitatively measure the level of synchronization for each simulation, we wrote code to output the synchronization index of V, [Ca], and [FBP] traces. To weigh the stiff and nonstiff regions of the oscillations equally in the index, we interpolated the data from the simulation using a time vector with equal spacing of 36ms per entry. A Pearson correlation is then run on the matrix containing all the V, [Ca], or [FBP] traces per simulation. We use the built-in Matlab function, `corr`, for the Pearson correlation. The (i, j) th entry of the resulting coefficient matrix is the Pearson coefficient for the i th and j th traces. We determine the index by taking the minimum average value of the rows. For this index we choose for what time period of each simulation to run the correlation. Since we are considering what pattern the simulation settle into, we typically run our SI on the last fifteen minutes of the simulation.

4 Results

Our simulations examined the behavior of voltage, calcium, and FBP under varying parameters and between heterogeneous groups of cells representing an islet. Our results show simulations of varying J_{GK} values in the CaI, CaD, and mixed CaI and CaD ranges, as well as varying levels of calcium coupling and voltage coupling.

4.1 Time Study

We did a time study in order to compare the use of the Matlab solver ode15s versus the modified ode15s version. Note that this time study was performed before we implemented the TIL. We found we could model larger amounts of cells without running out of memory (O.M.) using the Modified ode15s; however, the time saving effects of the Modified ode15s solver are minimal.

N	ode15s		Modified ode15s	
	0 pS	10 pS	0 pS	10 pS
2	1173	265	1159	263
3	2387	345	2288	338
4	O.M.	493	2908	466
5	O.M.	947	3376	844
6	O.M.	O.M.	4167	1180
7	O.M.	O.M.	O.M.	1768
8	O.M.	O.M.	O.M.	2693
9	O.M.	O.M.	O.M.	4288
10	O.M.	O.M.	O.M.	O.M.

Table 4.1: Simulations modeled the cells for one hour, homogeneous, a J_{GK} value of $0.18\mu\text{M}\cdot\text{ms}^{-1}$, and perturbed initials conditions with either voltage coupling or no coupling.

4.2 Adding Dz

We began by investigating CaI versus CaD modes. We added diazoxide (Dz) twenty minutes into an hour long simulation. Dz locks the K_{ATP} channels open, thus keeping the cell from depolarizing. Therefore, the Ca^{2+} channel cannot open and Ca^{2+} cannot enter the cell. When Dz is added, as seen in Figures 4.1a and 4.1b, Ca^{2+} oscillations terminate. Additionally, in the CaD mode, Figure 4.1b, the metabolic oscillations terminate; however, in the CaI mode seen in Figure 4.1a, the metabolic oscillations continue.

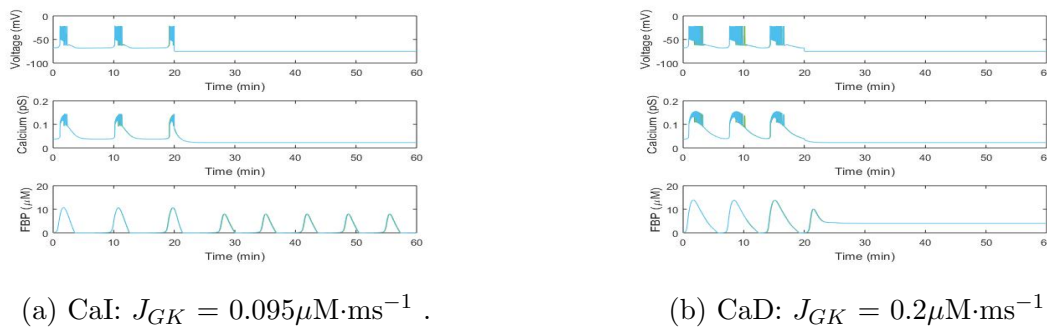


Figure 4.1: Simulations using $5\times 5\times 5$ block of cells, homogeneous, no-coupling, and adding Dz at 20 minutes.

4.3 Coupling Trends

Next we considered coupling in the CaD and CaI modes. Figures 4.2a and 4.2b, show that in the CaI modes, as voltage coupling increases, synchronization increases. Figures 4.3a and 4.3b demonstrate that for CaD modes, increasing voltage coupling seems to increase synchronization when making a visual comparison.

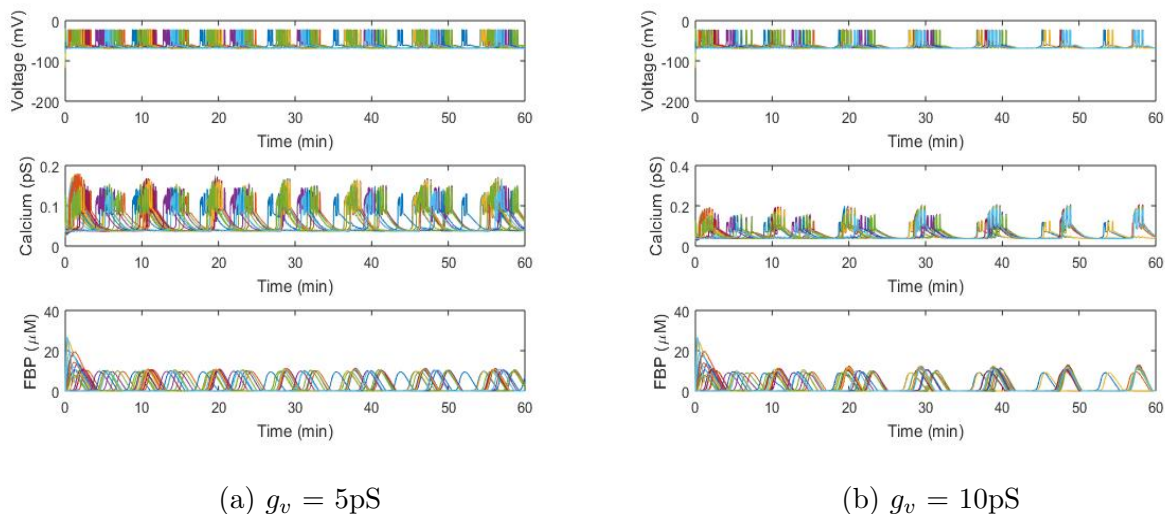


Figure 4.2: CaD runs with a J_{GK} value of $0.095\mu\text{M}\cdot\text{ms}^{-1}$, a $3\times 3\times 3$ block of cells, homogeneous, $g_{Ca} = 0\text{ms}^{-1}$ and the initial conditions are perturbed.

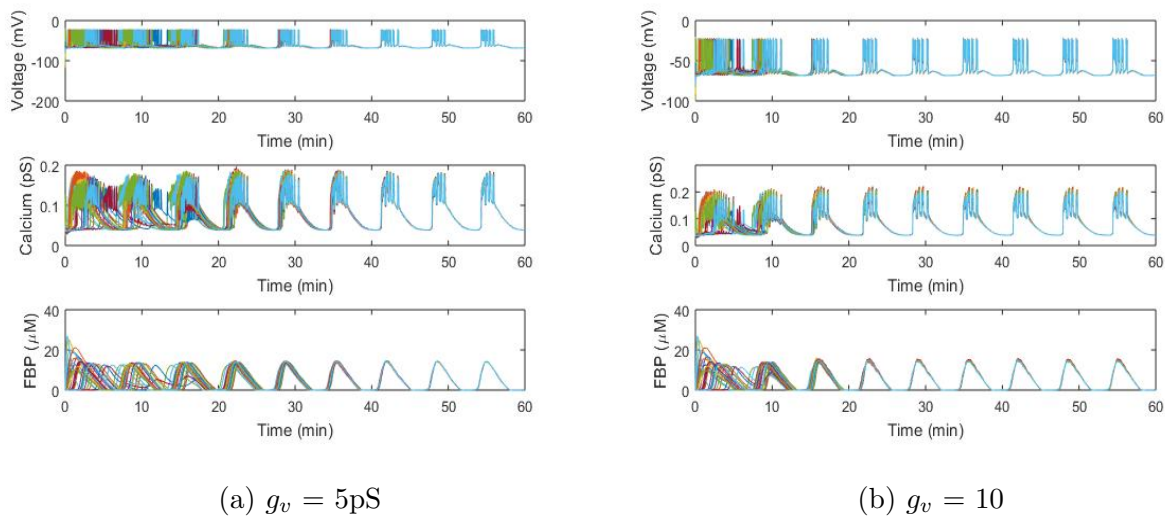


Figure 4.3: CaD runs with a J_{GK} value of $0.18\mu\text{M}\cdot\text{ms}^{-1}$, a $3\times 3\times 3$ block of cells, homogeneous, $g_{Ca} = 0\text{ms}^{-1}$ and the initial conditions are perturbed.

Increasing calcium coupling when the calcium coupling value is greater than 0.045ms^{-1} , does not have a significant effect on synchronization when making a visual comparison in both CaD and CaI modes as shown by Figure 4.4a compared to Figure 4.4b and Figure 4.5a compared to Figure 4.5b.

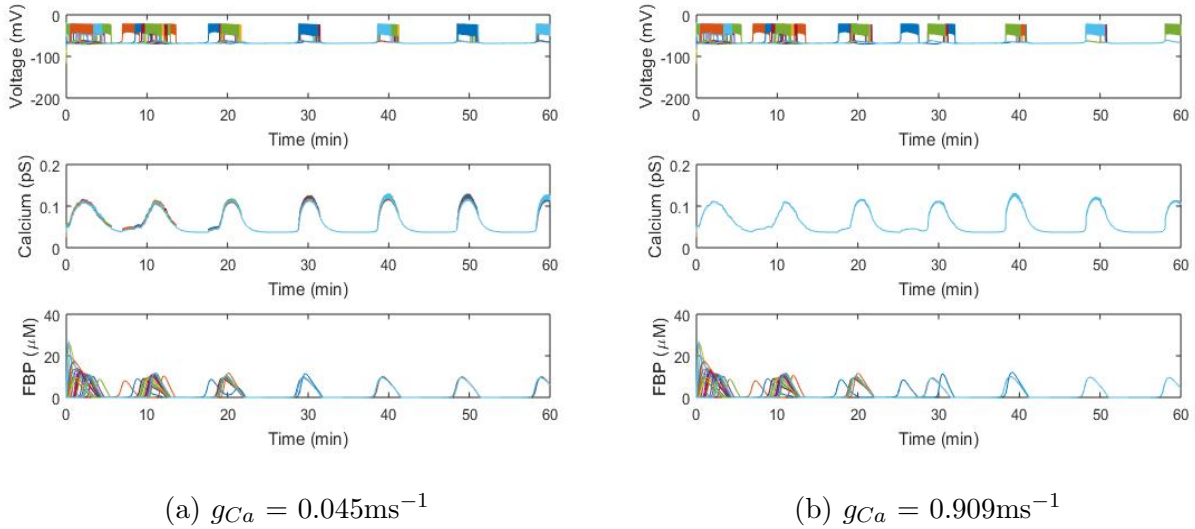


Figure 4.4: CaI runs with a J_{GK} value of $0.095\mu\text{M}\cdot\text{ms}^{-1}$, with a $3\times 3\times 3$ block of cells, are homogeneous, $g_v = 0\text{pS}$, and the initial conditions are perturbed.

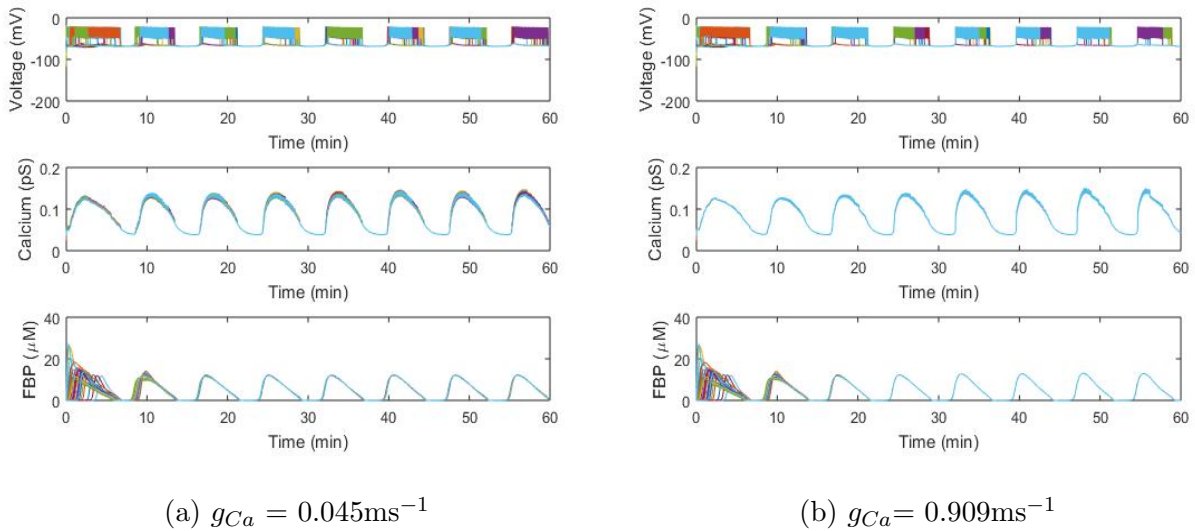


Figure 4.5: CaD runs with a J_{GK} value of $0.18\mu\text{M}\cdot\text{ms}^{-1}$, with a $3\times 3\times 3$ block of cells, are homogeneous, $g_v = 0\text{pS}$, and the initial conditions are perturbed.

When calcium coupling values are less than 0.045ms^{-1} , there is greater synchronization as the calcium values increase in both CaD and CaI modes as shown by Figures 4.6 and 4.7.

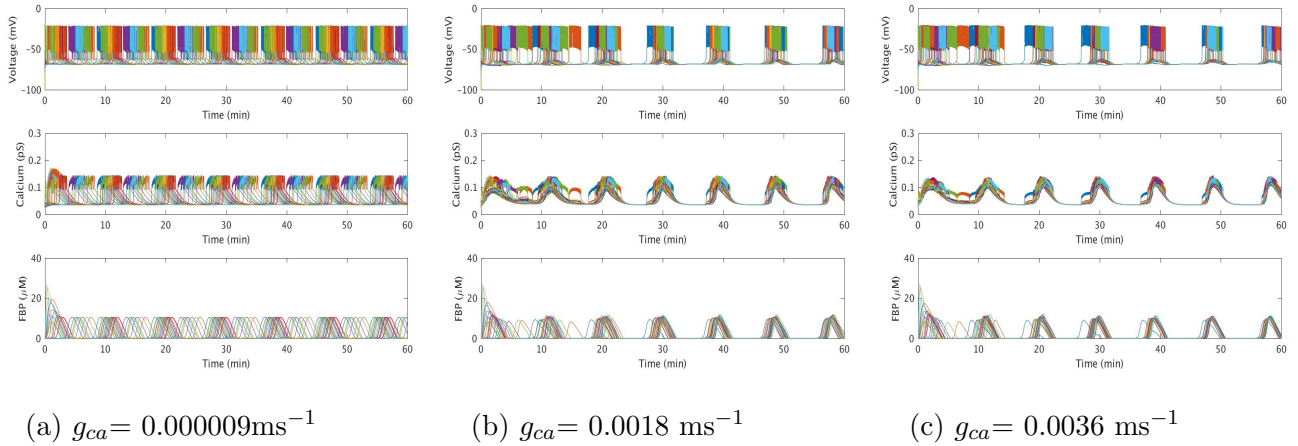


Figure 4.6: CaI runs with a J_{GK} value of $0.095\mu\text{M}\cdot\text{ms}^{-1}$, with a $3\times 3\times 3$ block of cells, are homogeneous, $g_v = 0\text{pS}$, and the initial conditions are perturbed.

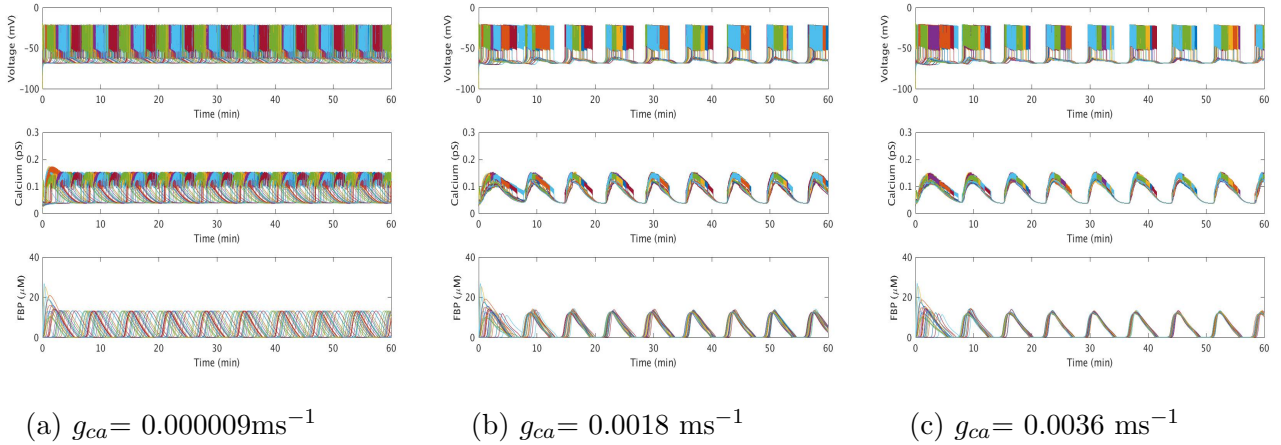


Figure 4.7: CaD runs with a J_{GK} value of $0.018\mu\text{M}\cdot\text{ms}^{-1}$, with a $3\times 3\times 3$ block of cells, are homogeneous, $g_v = 0\text{pS}$, and the initial conditions are perturbed.

4.4 Heterogeneity

We tested three different types of heterogeneity patterns with various pairs of J_{GK} values and various calcium and voltage coupling values. We found the differences between the three heterogeneity patterns to be small as seen in Figures: 4.8, 4.9, and 4.10.

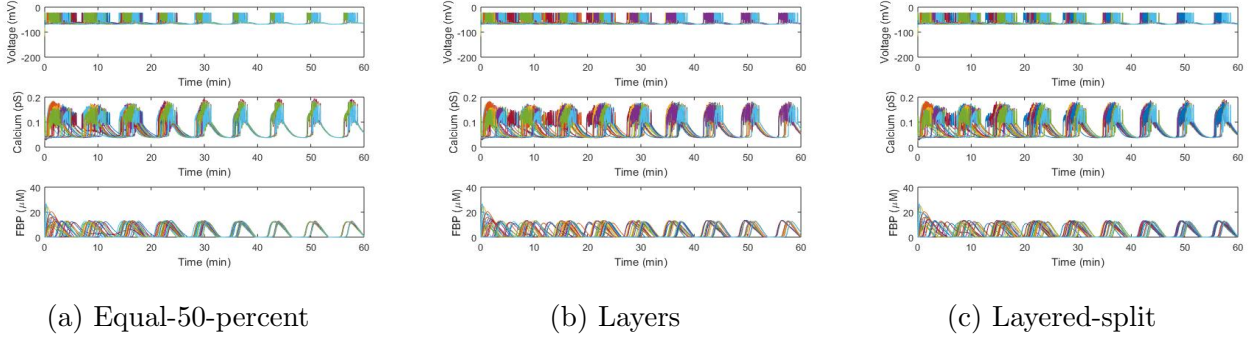


Figure 4.8: Mixed CaD and CaI with J_{GK} values of 0.14 and $0.18\mu\text{M}\cdot\text{ms}^{-1}$, with a $3\times 3\times 3$ block of cells, $g_v=5\text{pS}$, $g_{Ca}=0\text{ms}^{-1}$, and the initial conditions are perturbed.

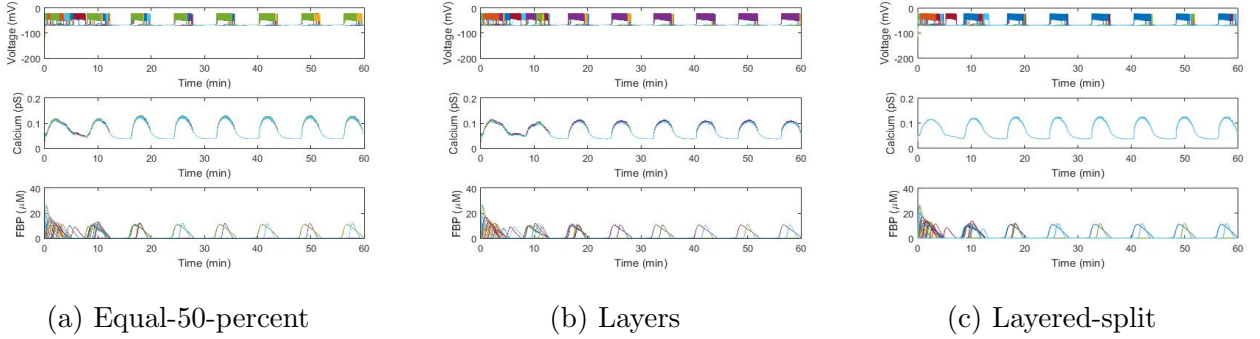


Figure 4.9: CaI pairs with J_{GK} values of 0.05 and $0.14\mu\text{M}\cdot\text{ms}^{-1}$, with a $3\times 3\times 3$ block of cells, $g_v=0\text{pS}$, $g_{Ca}=0.045\text{ms}^{-1}$, and the initial conditions are perturbed.

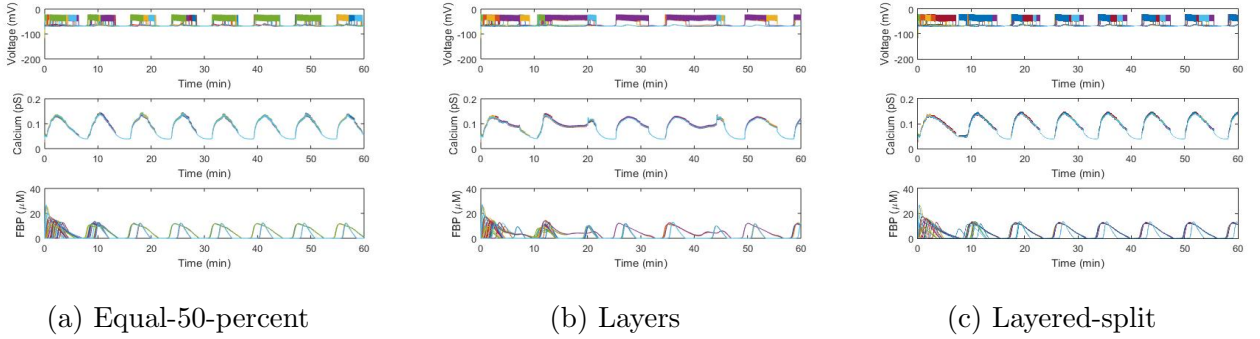


Figure 4.10: Mixed CaI and CaD pairs with J_{GK} values of 0.095 and $0.2\mu\text{M}\cdot\text{ms}^{-1}$, with a $3\times 3\times 3$ block of cells, $g_v=5\text{pS}$, $g_{Ca}=0.045\text{ms}^{-1}$, and the initial conditions are perturbed.

4.5 Synchronization

In order to quantify synchronization, we created a plot of the synchronization index (SI) for a set of simulations with varying parameters. Simulations were run with either the same or perturbed initial conditions as well as for a time period of one or two hours. Note that we apply the SI to the last fifteen minutes of each simulation. Each chart consists of twelve scatter plots with each plot representing a different voltage and calcium coupling combination. The x-axis shows the pairs of J_{GK} values while the y-axis represents the SI values. To represent the SI values of voltage, calcium, and FBP per simulation, each point is given a certain shape and color, voltage synchronization is a pink triangle, calcium synchronization a green circle, and FBP synchronization a blue X as seen in the legend, Figure 4.11. An SI value of one represents complete synchronization.



Figure 4.11: SI Legend

4.5.1 Synchronization Index Charts

In the synchronization index chart, we can see the trends as we change parameters. Each column of graphs represents a specific voltage coupling, which increases from left to right. Rows of graphs represent a given calcium coupling increasing from top to bottom. The first three columns in each graph have cells with J_{GK} values all in the CaI range. The next four columns have one J_{GK} value in the CaI range and one in CaD. The last three columns have J_{GK} values both in the CaD range. These different columns are designated by dashed lines.

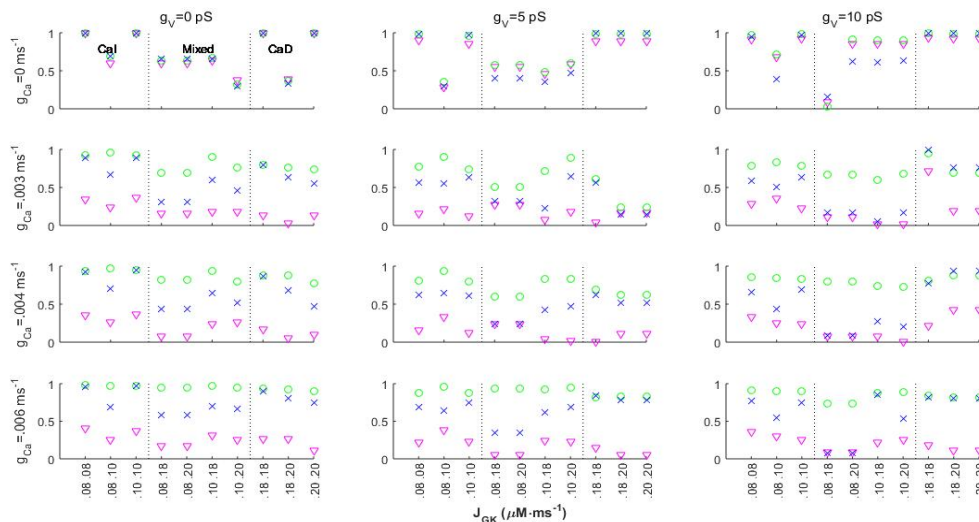


Figure 4.12: Simulations run with a $5 \times 5 \times 5$ cube, the same initial conditions, and the equal-50-percent bursting pattern for one hour.

In Figure 4.12 after an hour even a small amount of calcium coupling tends to cause voltage desynchronization. After two hours considering Figure 4.13 in comparison to Figure 4.12 in the mixed pairs of J_{GK} , the synchronization decreases for all of the calcium coupling strengths.

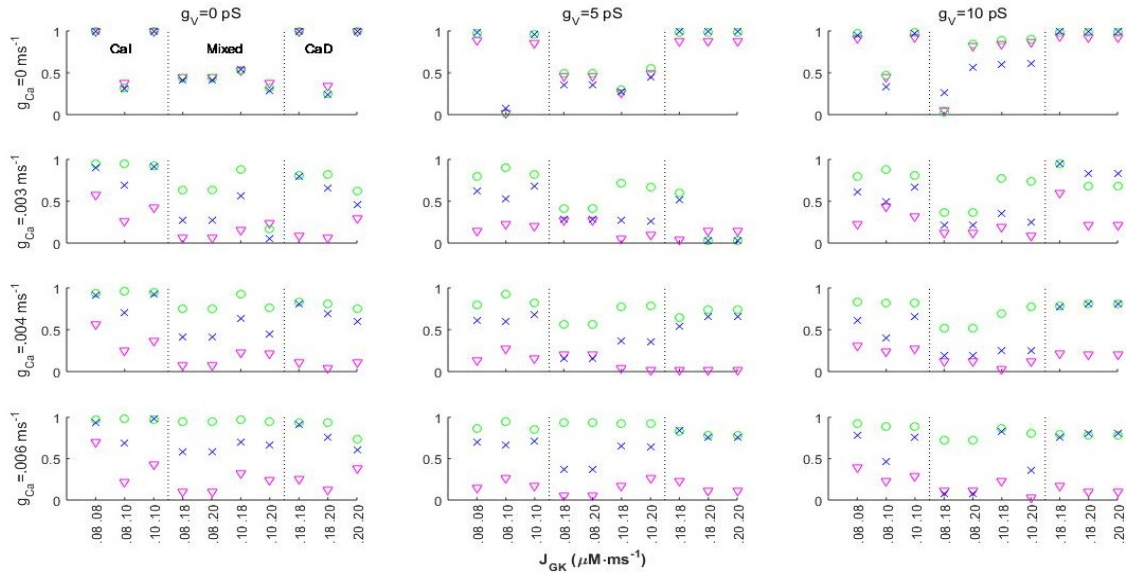


Figure 4.13: Simulations run with a $5 \times 5 \times 5$ cube, the same initial conditions, and the equal-50-percent bursting pattern for two hours.

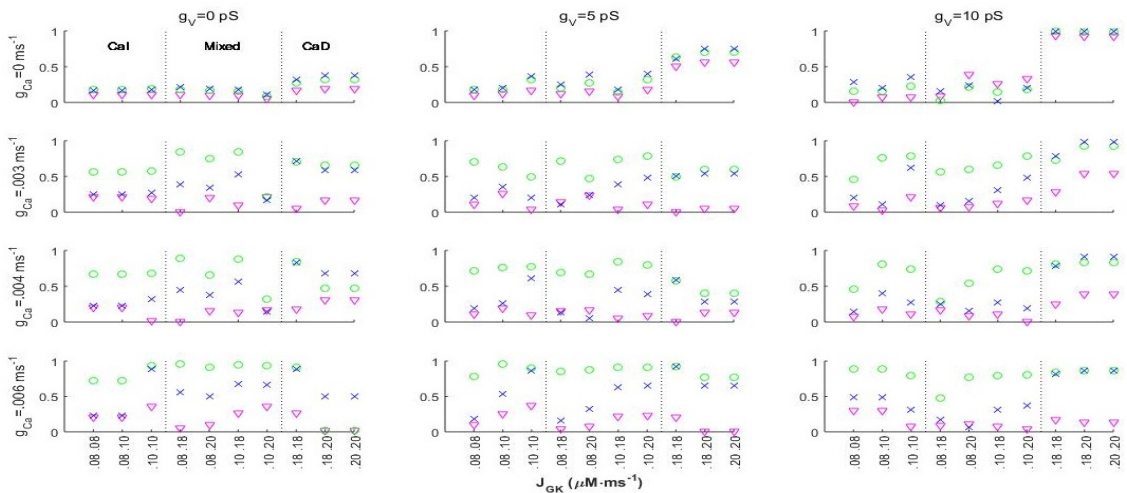


Figure 4.14: Simulations were run for one hour with a $5 \times 5 \times 5$ cube of cells, the equal-50-percent bursting pattern, and the initial conditions are perturbed.

We perturbed the initial conditions in Figure 4.14 and Figure 4.15. In comparing these figures, we observe that there are some instances of desynchronization when the simulations are run for two hours.

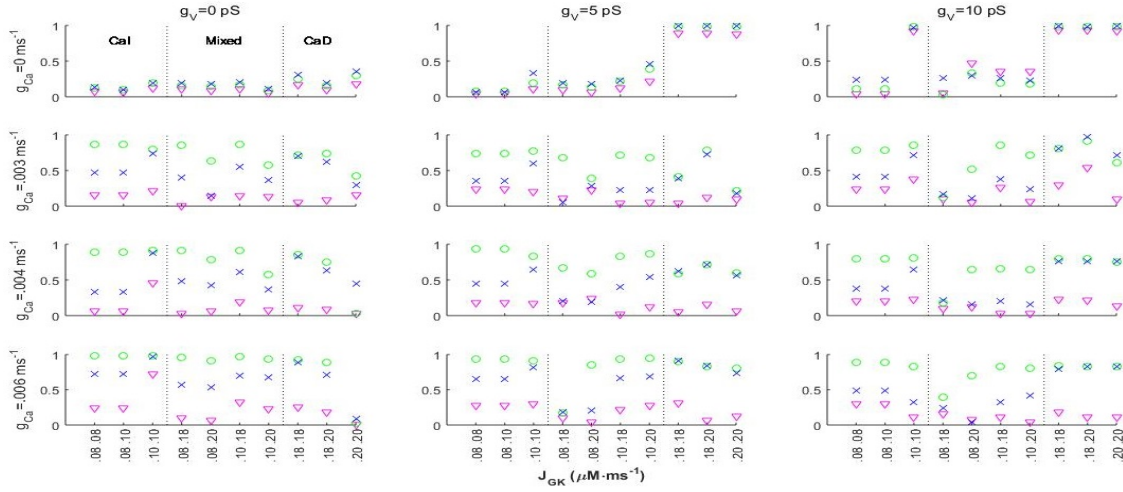


Figure 4.15: Simulations were run for one hour with a $5 \times 5 \times 5$ cube of cells, the equal-50-percent bursting pattern, and the initial conditions are perturbed.

4.5.2 Synchronization Trends Trend

We can deduce from the SI plot in Figure 4.14, that increasing voltage coupling in the CaD mode increases synchronization in all three oscillations, voltage, calcium, and FBP. Figures 4.16a through 4.16c demonstrates the trend of synchronization as voltage increases.

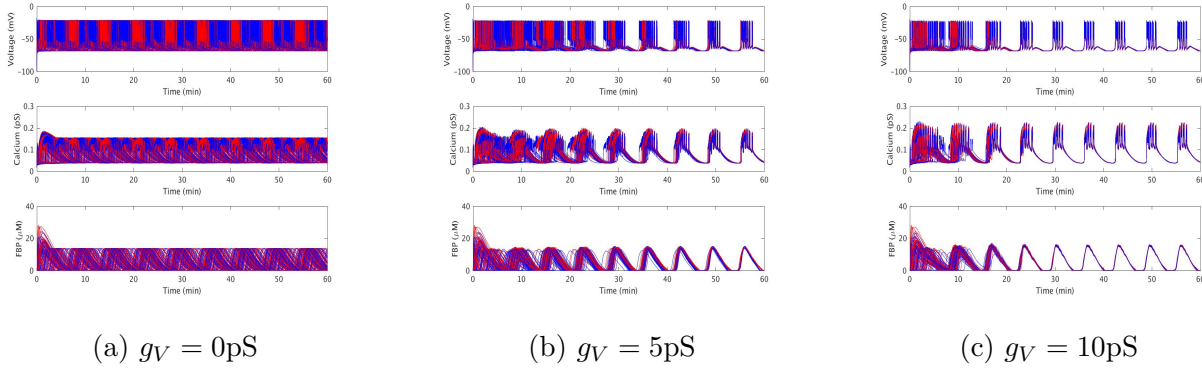


Figure 4.16: Simulations with a $5 \times 5 \times 5$ block of cells, $g_{Ca} = 0 \text{ms}^{-1}$, $J_{GK} = 0.18 \mu\text{M}\cdot\text{ms}^{-1}$ (blue) or $J_{GK} = 0.20 \mu\text{M}\cdot\text{ms}^{-1}$ (red), and the initial conditions are perturbed.

Another noticeable trend drawn from Figure 4.14 is that in CaI mode, increasing calcium coupling increases synchronization of all three oscillations, voltage, calcium, and FBP. Figure 4.17 shows the increasing trend of synchronization as the strength of the calcium coupling increases.

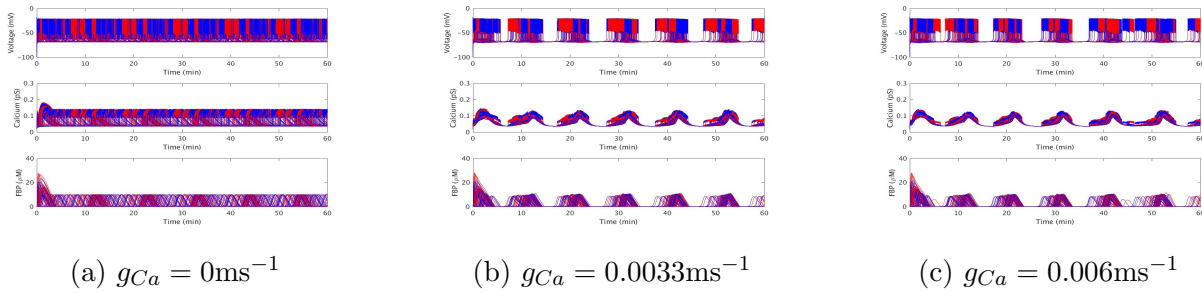


Figure 4.17: Simulations with a $5 \times 5 \times 5$ block of cells, $g_V = 0\text{pS}$, $J_{GK} = 0.08\mu\text{M}\cdot\text{ms}^{-1}$ (blue) or $J_{GK} = 0.10 \mu\text{M}\cdot\text{ms}^{-1}$ (red), and the initial conditions are perturbed.

4.5.3 Desynchronization

We observed from our the SI plot in Figure 4.14, that in certain cases, coupling can desynchronize the oscillations. We will compare the noticeable desynchronization cases in the following graphs.

The first desynchronization case is observed in simulations of CaD modes, where increasing calcium coupling desynchronizes voltage as seen in Figure 4.18.

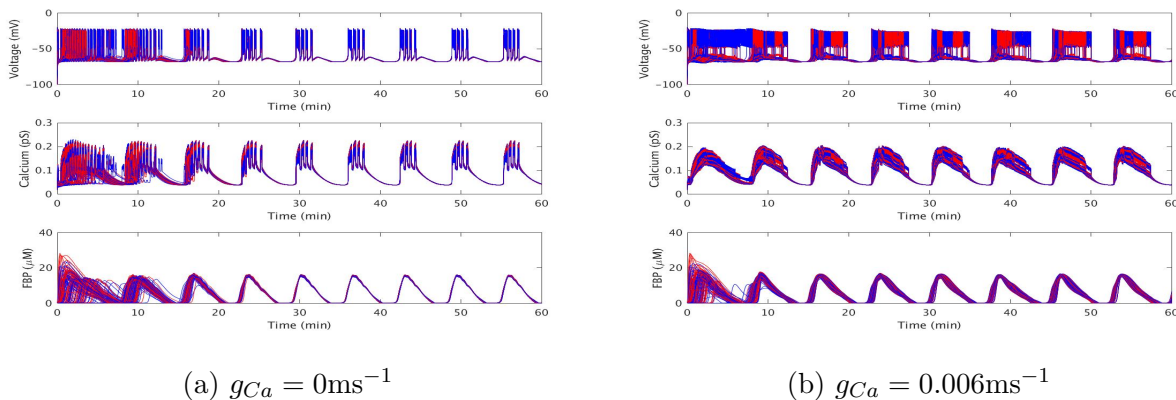


Figure 4.18: Simulations with a $5 \times 5 \times 5$ block of cells, $g_V = 10\text{pS}$, $J_{GK} = 0.18\mu\text{M}\cdot\text{ms}^{-1}$ (blue) or $J_{GK} = 0.20 \mu\text{M}\cdot\text{ms}^{-1}$ (red), and the initial conditions are perturbed.

We also see this desynchronization through the synchrony values as seen in Table 4.2.

SI	4.18a	4.18b
V	0.930	0.139
Ca ²⁺	0.987	0.866
FBP	0.997	0.862

Table 4.2: SI Values for Figures 4.18a and 4.18b

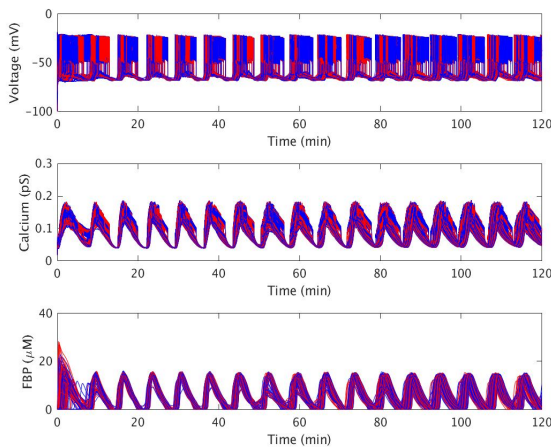
The next desynchronization case is observed when comparing Figures 4.14 and 4.15. Desynchronization occurred over time when both voltage and calcium were coupled and in the high end of the CaD region. In Figure 4.19a, calcium and FBP start to desynchronize around 40 minutes. We also see this desynchronization through the synchrony values as seen in Table 4.3. When we increase the calcium coupling strength in Figure 4.19b, the oscillations start desynchronizing around 40 minutes but re-synchronizes around 80 minutes. This is also apparent in its synchrony indices as seen in Table 4.4.

SI	1 hr	2 hr
Ca ²⁺	0.603	0.220
FBP	0.537	0.185

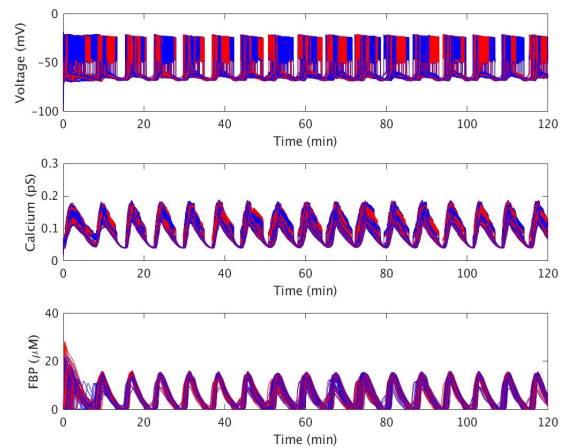
Table 4.3: SI Values for Figure 4.19a

SI	1 hr	2 hr
Ca ²⁺	0.406	0.602
FBP	0.285	0.567

Table 4.4: SI Values for Figure 4.19b



(a) $g_{Ca} = 0.003\text{ms}^{-1}$



(b) $g_{Ca} = 0.004\text{ms}^{-1}$

Figure 4.19: Simulations with a $5 \times 5 \times 5$ block of cells, $g_V = 5\text{pS}$, $J_{GK} = 0.20\mu\text{M}\cdot\text{ms}^{-1}$ (blue and red), and the initial conditions are perturbed.

The following desynchronization case is when the FBP oscillations stop over time. We observed this case for simulations with calcium coupling only, in CaD mode of high J_{GK} values. Figure 4.20 demonstrates this desynchronization, where the graph of FBP oscillations become flat around 100 minutes. Note that calcium has small fast oscillations mirroring the fast spiking electrical oscillations.

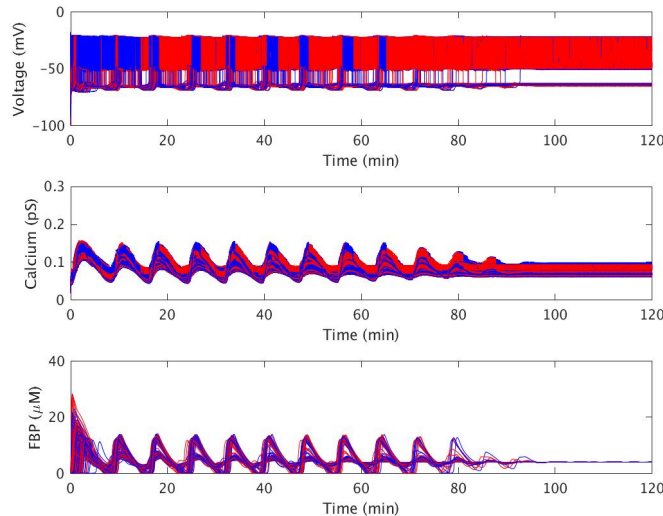


Figure 4.20: Simulations with a $5 \times 5 \times 5$ block of cells, $g_V = 0\text{pS}$, $g_{Ca} = 0.004\text{ms}^{-1}$, $J_{GK} = 0.20\mu\text{M}\cdot\text{ms}^{-1}$ (blue and red), and the initial conditions are perturbed.

4.6 Future Research

The memory issue that arises when running large numbers of cells is that output from the ODE solver, which contains the information needed for graphing, is not written to the Matlab file when the amount of data is too large. We were able to overcome this by using a Time Interval Loop (TIL), which is the loop we implemented based on a chosen time which writes the information to multiple files. Although our solution works, it requires the time period to be manually selected in order for the file to be under a size limit. For example, thirty minute periods typically work for a $3 \times 3 \times 3$ case whereas the time period needs to be reduced to fifteen minutes for a $5 \times 5 \times 5$ model. However, this can vary due to different amounts and types of coupling and the amount of perturbation of the initial conditions. A method to solve the issue of choosing a sufficient time would be to create a loop in the ODE solver based on the number of steps. We found that you can take a certain amount of steps before running out of memory. If new files were written based on this number of steps, then a greater number of cells could be simulated without running out of memory and without having to test to find an appropriate time. Additionally, a time study could be performed considering

the code before the TIL, the code with our optimization loop, and the code implementing the loop based on number of steps.

5 Conclusion

We used the Dual Oscillator Model and the modified ODE solver to better understand the role of calcium oscillations in CaI and CaD modes. In addition, we were able to create a synchronization index to demonstrate the trends in voltage and calcium coupling, as well as differing J_{GK} values. Through this, we were able to better study the impact of CaI, CaD, and mixed modes on oscillations. To improve simulations by modeling more cells in each simulation, the code was modified to write multiple MAT-files using a loop for a chosen time.

Coupling complex cells together has interesting dynamic effects. In CaI modes, increasing calcium coupling with no voltage coupling increases synchronization. In CaD modes, increasing voltage coupling with no calcium coupling increases synchronization as well. However, in CaD modes, voltage coupling with high calcium coupling causes desynchronization in voltage. This is reminiscent of the work on coupled cells [5], where adding calcium permeability between cells leads to a desynchronization of voltage via a pitchfork bifurcation. These results help us to better understand how calcium is organized in pancreatic islets in the process of insulin secretion.

References

- [1] Richard Bertram, Leslie Satin, Min Zhang, Paul Smolen, and Arthur Sherman. Calcium and glycolysis mediate multiple bursting modes in pancreatic islets. *Biophysical Journal*, 87:3074–3087, 2004.
- [2] George Eskandar, Jennifer Houser, Ellen Prochaska, Jessica Wojtkiewicz, Terasa Lehair, and Bradford E. Percy. Investigating how calcium diffusion affects metabolic oscillations and synchronization of pancreatic beta cells. Technical Report HPCF–2015–24, UMBC High Performance Computing Facility, University of Maryland, Baltimore County, 2014.
- [3] Christopher P. Fall. *Computational Cell Biology*. Springer, 2002.
- [4] Samuel Khuvis, Matthias K. Gobbert, and Bradford E. Percy. Time-stepping techniques to enable the simulation of bursting behavior in a physiologically realistic computational islet. *Mathematical Biosciences*, 263:1–17, 2015.
- [5] K Tsaneva-Atanasova, CL Zimlicki, R Bertram, and A Sherman. Diffusion of calcium and metabolites in pancreatic islets: killing oscillations with a pitchfork. *Biophysical Journal*, 90:3434–3046, 2006.

- [6] Margaret Watts, Bernard Fendler, Matthew J. Merrins, Leslie S. Satin, Richard Bertram, and Arthur Sherman. Calcium and metabolic oscillations in pancreatic islets: Who's driving the bus? *SIAM Journal on Applied Dynamical Systems*, 13(2):683–703, 2014.